

Parallel Augmentation and Dual Enhancement for Occluded Person Re-identification

Zi Wang,¹ Huaibo Huang,^{2,3} Aihua Zheng,^{4,5,6} Chenglong Li,^{4,5,6} Ran He^{2,3,*}

¹School of Computer Science and Technology, Anhui University

²Center for Research on Intelligent Perception and Computing, CASIA, Beijing, China

³National Laboratory of Pattern Recognition, CASIA, Beijing, China

⁴Anhui Provincial Key Laboratory of Multimodal Cognitive Computation

⁵Information Materials and Intelligent Sensing Laboratory of Anhui Province

⁶School of Artificial Intelligence, Anhui University

ziwang1121@foxmail.com, huaibo.huang@cripac.ia.ac.cn, {ahzheng214, lcl1314}@foxmail.com, rhe@nlpr.ia.ac.cn

Abstract

Occluded person re-identification (Re-ID), the task of searching for the same person's images in occluded environments, has attracted lots of attention in the past decades. Recent approaches concentrate on improving performance on occluded data by data/feature augmentation or using extra models to predict occlusions. However, they ignore the imbalance problem in the test set and not fully utilize the information from the training data. To alleviate the above problems, we propose a simple but effective method with **Parallel Augmentation and Dual Enhancement (PADE)** that is robust on both occluded and non-occluded data, and does not require any auxiliary clues. First, we design a parallel augmentation mechanism (**PAM**) for occluded Re-ID to generate more suitable occluded data to mitigate the negative effects of unbalanced data. Second, we propose the dual enhancement strategy (**DES**) for global and local features to promote the context information and details. Experimental results on widely used occluded datasets (Occluded-Duke, Partial-REID, and Occluded-ReID) and non-occluded datasets (Market-1501 and DukeMTMC-reID) validate the effectiveness of our method. The code will be available soon.

Introduction

On the basis of the non-occluded person Re-ID, the occluded person Re-ID, which incorporates the data obscured by various obstacles, has recently gained popularity due to its benefits for social security and vehicle monitoring.

The occlusions are uncommon in the training set (Zheng et al. 2015a; Miao et al. 2019a) but abundant in the test set (especially in query) as illustrated in the Fig.1 (a). Training with such unbalanced data makes improving the network's flexibility to unknown test data challenging. Efforts in data and feature augmentation are emerging to eliminate the imbalance between training and testing. Most methods (He et al. 2021; Sun et al. 2018; Zhou et al. 2019) employ standard data augmentation such as random flipping, random deleting, random cropping, and so on. Furthermore, FED (Wang et al. 2022c) provided feature augmentation strategies to improve the network's adaptability to occluded data. The widely used data/feature augmentation mechanisms take one image/feature as the input and

output only one changed image/feature to the subsequent network for training, as Fig. 2 (a) shows. We can see from Fig.1 (b) that practically all occlusions occur in the query, whereas the gallery images almost never have any obstructions in some occluded Re-ID dataset (Zheng et al. 2015b; Zhuo et al. 2018).

However, the methods that focus on data/feature augmentations often ignore the unbalanced occlusion between query and gallery (in testing phase). They can generate more data for training, but may not balance the occluded data and non-occluded data in each batch because the erase and crop operations are completely random. To increase the network's robustness on both the non-occluded data (in the gallery) and the occluded data (in the query), we design a novel data augmentation mechanism called the **Parallel Augmentation Mechanism (PAM)**. To alleviate this problem, we adjust existing data augmentation mechanisms to three independent augmentations, *BaseAugmentation*, *ErasingAugmentation*, and *CroppingAugmentation* for occluded Re-ID. We keep the erasing and the cropping operations to generate occlusions on input images. In our parallel augmentation mechanism, *ErasingAugmentation* only implements the erase operation, and *CroppingAugmentation* only crops the original image. In contrast to the existing augmentation, both erase and crop operations will be executed in the preprocessing phase, as illustrated in Fig. 2 (b). We will obtain an image triplet (including two augmented and one original non-occluded image) after the parallel augmentation, and the ViT-based feature extractor takes the image triplet as the input as shown in Figure 3.

Additionally, both details and context information are crucial for occluded person Re-ID, they have their own advantages in different situations. As illustrated in Fig. 1 (c), we can simply identify *ID1* and *ID2* by local details while finding it hard to distinguish them based on their outward appearance. (Song et al. 2018; Gao et al. 2020; Wang et al. 2022a) proposed using additional clues to leverage foreground segmentation and pose estimation models to extract body parts and predict the locations of occlusions when global features are polluted. The methods without using extra models or annotations usually focus on extracting dis-

*Corresponding author

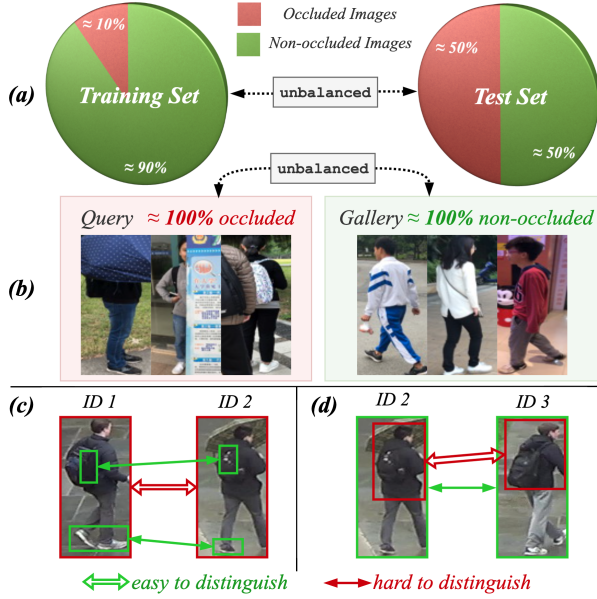
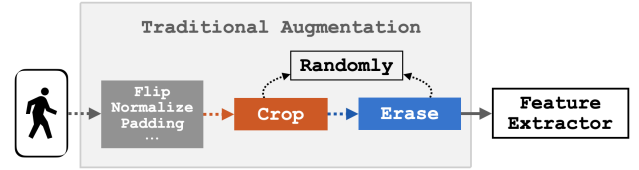


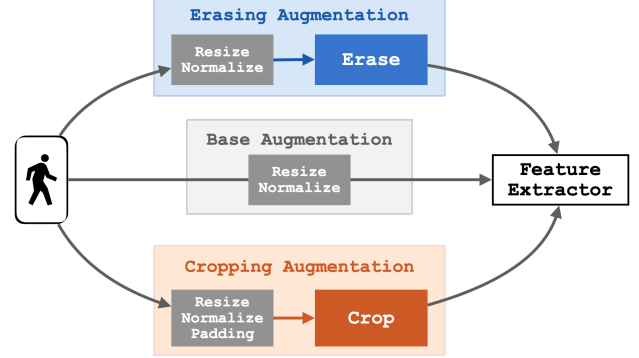
Figure 1: a) Compared to the training set (Zheng et al. 2015a), the test sets (Zheng et al. 2015b; Zhuo et al. 2018) have a significantly higher percentage of occluded samples. b) The images in the gallery are almost exclusively non-occluded, whereas the images in the query are almost all occluded. c) Pedestrians who appear to be the same at first glance but differ in local details. d) Despite many similarities, the two pedestrians can be clearly distinguished from one another.

criminative description from local and global features. Part-based methods (Sun et al. 2018; Wang et al. 2018, 2022b) proposed to split the global feature into several parts, and use finer features that contain detailed information for training. And the global information becomes more crucial when the body is hindered by unknown impediments or the details are similar as shown in Fig.1 (d). ViT-based approaches (He et al. 2021; Wang et al. 2022c,a) proposed using ViT as a feature extractor due to the extreme sensitivity of global information.

However, when encountering new datasets, the methods using auxiliary clues are susceptible and require extra annotations and fine-tuning. And while the different persons have similar appearances, only using extracted local/global information or simply fusing context information and details is not discriminative enough. To make full use of the global and local features, we propose to enhance context information and details by forcing global and local features promote each other. Inspired by (Wang et al. 2022b), we propose the dual enhancement strategy (DES) on the global and local features extracted by our ViT-based backbone. As shown in Figure 3, the global and local features will be enhanced in two sequential steps. First, each local feature can be boosted by the context information in original global feature, and then the global feature can absorb the detailed information in the enhanced local features. It is worth noting that our DES



(a) The widely used data augmentation mechanism in Re-ID.



(b) The parallel augmentation mechanism in our method.

Figure 2: (a) The traditional augmentation implements crop and erase on the images, and then outputs an augmented image. (b) For each input, we perform both the erasing and cropping augmentations in parallel and finally feed it into the feature extractor along with the non-occluded image.

does not require additional annotation or model assistance.

In summary, we aim to improve the robustness of the network on both occluded and non-occluded data with no additional models or annotations. Our simple but effective baseline for occluded Re-ID consists of two key components: Parallel Augmentation Mechanism (PAM) and Dual Enhancement Strategy (DES).

- We design the Parallel Augmentation Mechanism for occluded Re-ID. All the non-occluded images, the images erased by *ErasingAugmentation* and the images cropped by *CroppingAugmentation* are sent to the feature extractor together to improve the robustness of the network in the training phase.
- We propose to enhance the global and local features according to the Dual Enhancement Strategy. All local features can be enhanced by the context information, and the global features can absorb the details from the boosted local features.
- Our method can improve the robustness of the model on both occluded and non-occluded data without any auxiliary clues. The experimental results on five widely used Re-ID datasets demonstrate the effectiveness and generality of the proposed methods.

Related Work

Occluded Person Re-ID

The main challenge in occluded Re-ID is the unknown occlusions in person images. Some methods (Wang et al. 2020;

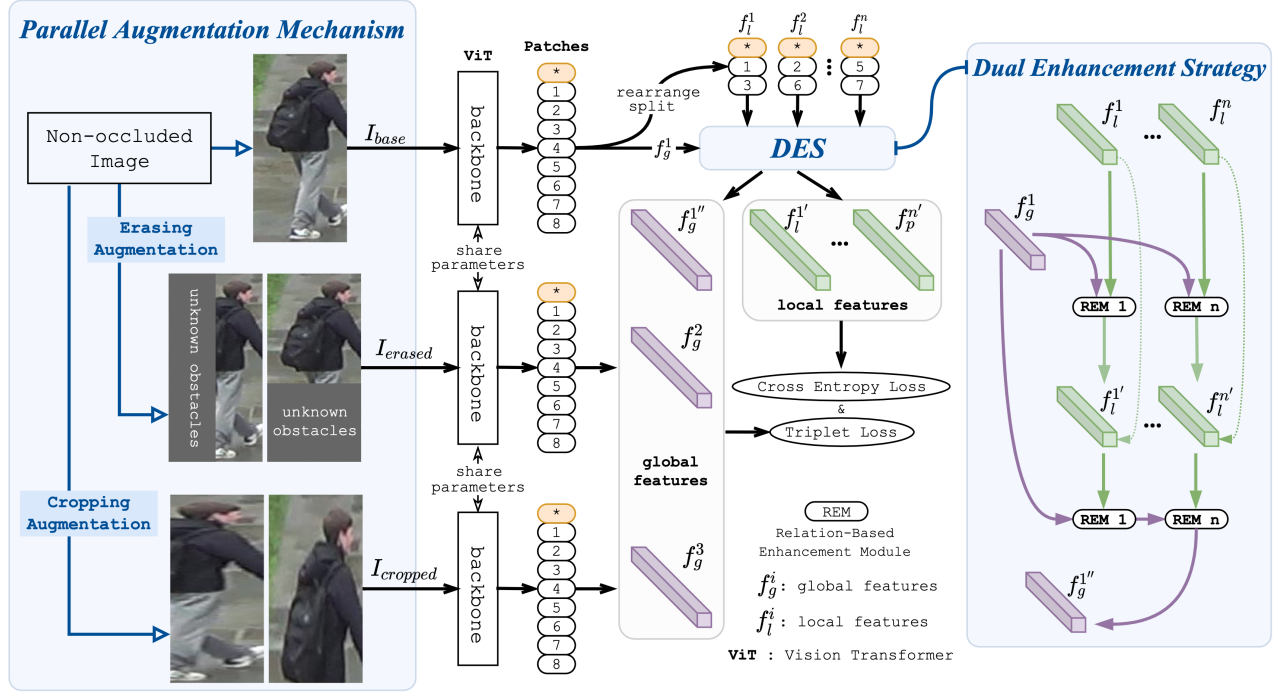


Figure 3: Overall structure of the proposed method. First, we implement erase and crop operations on original inputs to form the image triplet (Original, Erased, and Cropped images). And the image triplet will be sent to the ViT-based backbone to extract global features. Then the global and local features from the non-occluded image branch will be enhanced by each other in an interactive way. Finally, all global and local features are concatenated to form the person description. It is worth noting that three ViT-based backbones share the parameters in our method.

Gao et al. 2020; Wang et al. 2022a) proposed to use auxiliary clues like segmentation labels and pose keypoints. HOReID (Wang et al. 2020) proposed to align feature by joint high-order relation modeling and topology information. PFD (Wang et al. 2022a) proposed to leverage the feature matching and learning by introducing the pose-guided aggregation. But the model introducing extra clues will increase the time and memory occupation, and be sensitive to the pre-trained model or annotations. Therefore, some methods (Sun et al. 2019; Zhu et al. 2020) proposed to predict the locations of occlusion or the visibility scores of body parts without using outside cues. VPM (Sun et al. 2019) proposed to predict the visibility scores of every regions in the image, and ISP (Zhu et al. 2020) proposed to generate the pseudo labels of each body parts for person Re-ID. Recently, due to the strong ability of vision transformer (Dosovitskiy et al. 2020) to extract discriminative features, ViT-based methods (He et al. 2021; Li et al. 2021; Wang et al. 2022c,a) achieve high accuracy on person Re-ID.

Augmentations in Person Re-ID

The data augmentation is crucial for training robust models in computer vision. The widely used data transformation includes simple operations on input images like random horizontal flip, random erase, random crop, image normalization, and so on. In person Re-ID, almost all the baseline (Zhou et al. 2019; Sun et al. 2018; Ye et al. 2021) and im-

proved methods (Miao et al. 2019b; Wang et al. 2022a; Gao et al. 2020; Wang et al. 2020) sets data transformation as the necessary step in the data preprocessing. Specially, Luo et al. (2020) propose to mix data from different training set to smooth the transition between the source and the target domain, MID (Huang et al. 2022) proposed to mix different modality data in training phase to leverage the modality-shared information by implement widely used mixup (Zhang et al. 2017; Ding et al. 2022; Xu et al. 2020). Moreover, in occluded Re-ID, FED (Wang et al. 2022c) proposed the feature erasing to tackle the distractions from different occlusions. However, these augmentation methods ignore the unbalanced data in the test set, and fail to perform robustly on both non-occluded and occluded Re-ID.

Methods

In this section, we will introduce the proposed simple but effective baseline in detail. First, we introduce the Parallel Augmentation Mechanism (PAM) to generate an image triplet including non-occluded, erased, and cropped images. Second, we split the global feature from the non-occluded branch into several local features. Then we enhance both local and global in an interactive way by the proposed Dual Enhancement Strategy (DES). Finally, the enhanced global and local features will be concatenated to form the final description for Re-ID. The overall structure of our method is shown in Fig. 3.

Listing 1: Parallel Augmentation Mechanism

```

1 BaseAugmentation = Compose([
2     Resize(TrainSize),
3     ToTensor(),
4     Normalize()])
5
6 EraseAugmentation = Compose([
7     Resize(TrainSize),
8     ToTensor(),
9     Normalize(),
10    RandomErasing(probability=1)])
11
12 CropAugmentation = Compose([
13     Resize(TrainSize),
14     Pad(30),
15     ToTensor(),
16     Normalize(),
17     RandomResizedCrop(size=TrainSize)])

```

Parallel Augmentation Mechanism

In order to better train the network to adapt to the Re-ID task, almost all approaches will implement data augmentation in the preprocessing phase. The most widely used data augmentations in Re-ID are random horizontal flip, zero pad, random erase, and random crop. However, these augmentations are performed randomly and in a serial manner, as shown in Fig. 2. Occluded person Re-ID aims to match non-occluded and occluded images of the same person in the testing phase. The existing data augmentations are still insufficient in improving the robustness of the network to different occluded images of the same person. To alleviate the mentioned problem, we design the parallel augmentation mechanism (PAM) for occluded person Re-ID, which generates augmented images in a parallel manner and finally forms an image triplet for subsequent network.

For every input image I , we first implement two augmentations on it to obtain the image triplet $[I_{base}, I_{erased}, I_{cropped}]$ for training. This process can be formulated as:

$$\begin{aligned}
 I_{base} &= \text{BaseAugmentation}(I), \\
 I_{erased} &= \text{ErasingAugmentation}(I), \\
 I_{cropped} &= \text{CroppingAugmentation}(I).
 \end{aligned} \tag{1}$$

We keep the normalization operation in all three augmentations. Compared to traditional data preprocessing, the *BaseAugmentation* only change the size of the input image, the *ErasingAugmentation* only add obstacles at random locations on the image, and the *CroppingAugmentation* only crop the image irregularly. It is worth noting that the random horizontal flip operation is not included in our parallel augmentation because it may destroy the orientation consistency of the image triples fed into the network. After parallel augmentation, we obtain one image similar to the non-occluded image and two generated images with different types of occlusion. Then, all three images will be sent to a parameter-shared multi-branch network. In our method, we choose the feature extractor in TransReID as our backbone due to its powerful ability.

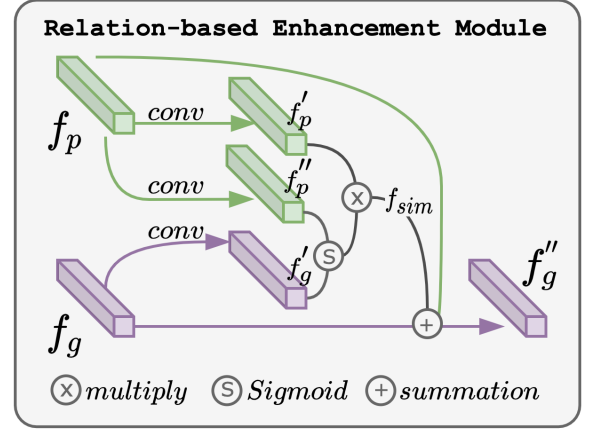


Figure 4: Structure of relation-based enhancement module. Take the single local feature f_l enhance the global feature f_g for example.

Dual Enhancement Strategy

The context information (in global feature) and details (in local feature) are critical in person Re-ID. Many approaches extract both global and local feature in training phase and optimize them together. However, they ignore the context information and details may not be valid at the same time, as shown in Fig. 1 (c). Therefore, we propose to enhance both global and local features in training phase in the interactive way. Inspired by the interaction of global and local features in multi-modal person Re-ID (Wang et al. 2022b), we design a dual enhancement strategy for occluded Re-ID.

After feature extraction, we can obtain three global features (f_g^1, f_g^2, f_g^3) from $I_{base}, I_{erased}, I_{cropped}$ respectively. Due to the $I_{erased}, I_{cropped}$ are polluted by unknown obstacles and irregular crop, the local details of global feature f_g^2 and f_g^3 have limited useful information. Therefore, only the global feature f_g^1 from I_{base} processed by *BaseAugmentation* and corresponding local features ($f_l^1, f_l^2 \dots f_l^n$) are considered in our dual enhancement strategy. The n denotes the number of local features, and set to 4 in experiment. First, each local feature will be enhanced by global feature, and the original local features are treated as residuals and added back to the enhanced local features. This process can be formulated as follow:

$$f_l^{i'} = \text{REM}(f_l^i, f_g^1) + f_l^i, \quad i = 1, \dots, n \tag{2}$$

Then the global features are also enhanced in the same way to absorb the details in the local features, as shown in Fig. 3. This process can be formulated as:

$$\begin{aligned}
 f_g^{1''} &= \text{REM}(f_g^1, f_l^i), \quad i = 1 \\
 f_g^{i''} &= \text{REM}(f_g^i, f_l^i), \quad i = 2, \dots, n
 \end{aligned} \tag{3}$$

The REM denotes relation-based enhancement module as shown in Fig. 4, and can be formulated as:

$$\begin{aligned}
 f_{sim} &= \text{Sigmoid}(f_l^i \odot f_g^i) * f_l^i, \\
 f_g^{i'} &= f_{sim} + f_g^i + f_l^i,
 \end{aligned} \tag{4}$$

Methods	Auxiliary Clues	Backbone	Occluded-Duke		Partial-REID		Occluded-ReID	
			mAP	Rank-1	mAP	Rank-1	mAP	Rank-1
HOReID	✓	CNN	43.8	55.1	-	85.3	70.2	80.3
PVPM	✓	CNN	-	-	72.3	78.3	61.2	70.4
PFD	✓	ViT	61.8	69.5	-	-	83.0	81.5
PCB	×	CNN	33.7	42.6	63.8	66.3	28.9	41.3
PGFA	×	CNN	37.3	51.4	61.5	69.0	-	-
OAMN	×	CNN	46.1	62.6	77.4	86.0	-	-
MoS	×	CNN	49.2	61.0	-	-	-	-
ISP	×	CNN	52.3	62.8	-	-	-	-
ViT Base	×	ViT	52.3	59.9	74.0	73.3	76.7	81.2
PAT	×	ViT	53.6	64.5	-	88.0	72.1	81.6
FED	×	ViT	56.4	68.1	80.5	83.1	79.3	86.3
TransReID	×	ViT	59.2	66.4	-	-	-	-
Ours	×	ViT	63.0	72.3	84.8	89.3	79.9	83.7

Table 1: Experimental results on Occluded-Duke, Partial-REID and Occluded-ReID compared with state-of-the-art CNN-based and ViT-based methods (in %). The best results are shown in **bold**, the second results are shown in **blue**.

where the f'_l , f''_l and f'_g are the features after $Conv1 \times 1$, the \odot denotes transpose multiply. The structure of REM is shown in Fig. 4, and we use only one local feature and the global feature to illustrate. After dual enhancement, both global and local features contain information from context and details. Then all global features (f_g^1, f_g^2, f_g^3) and local features (f_l^1, \dots, f_l^n) will be concatenated to form the final person description for training, and only f_g^1 and corresponding local features will be used in testing phase.

The main difference of our dual enhancement strategy and interaction in (Wang et al. 2022b) is that we consider both context and detailed information in person Re-ID, and the global and local features will promote each other in our DES. (Wang et al. 2022b) only used the global information to enhance local features, ignoring the importance of local details.

Loss Function

We choose the cross entropy loss as the identity loss (L_{id}) to train classifiers in our experiment. We adopt the triplet loss (L_{tri}) to enlarge the distances of different person and cluster features belonging to the same identity. All the global and local features are under the constraint of L_{id} and L_{tri} . The final loss function can be formulated as:

$$Loss_{final} = L_{cls} + L_{metric}, \quad (5)$$

where L_{cls} is the summation of all cross entropy losses and L_{metric} is the summation of all triplet losses. In our training phase, the computation of L_{cls} and L_{metric} can be formulated as:

$$L_{cls} = L_{id}(\Theta(f_g^{1''}), y) + \sum_{i=2}^3 (L_{id}(\Theta(f_g^i), y)) + \sum_{j=1}^n (L_{id}(\Theta(f_l^{j'}), y)) \quad (6)$$

$$L_{metric} = L_{tri}(f_g^{1''}) + \sum_{i=2}^3 L_{tri}(f_g^i) + \sum_{j=1}^n L_{tri}(f_l^{j'}) \quad (7)$$

where the Θ denotes the probability prediction function consists of a bottleneck layer and a fully connected layer. The y denotes the ground truth of each sample. The $f_g^{1''}$ denotes the global feature of non-occluded image, the f_g^i denotes the global feature of erased/cropped images, the $f_l^{j'}$ denotes the enhanced local feature. The n denotes the number of local features, and $n = 4$ in our experiment.

Implementation Details

The implementation platform of our experiment is Pytorch with RTX 3090Ti GPUs. The basic framework of our method is the ViT-based baseline TransReID (He et al. 2021), the original learning rate is set as 0.008, and will be reduced in epoch 40 and 70. The max epoch is 170, the batch size is set to 32, our model will occupy about 17GB GPU memory. All the global and local features are under the constraints of cross-entropy and triplet loss. In the training phase, the network will output three global features and four local features. Since the parameters of the three branches are shared, we only concatenate one global feature and four local features for testing, the dimension of final person description is $768 * (1 + 4) = 3840$ -dim. The Stochastic Gradient Descent (SGD) with the weight decay of 0.0004 is used in our experiment to fine-tune the whole network.

Experiment

In this section, we show several experimental results of the proposed method and state-of-the-art (SOTA) approaches on different datasets, including widely used non-occluded and occluded datasets. First, we introduce all the datasets used in detail. Then we compared our method with SOTA approaches on both part and all occluded. Then we show the

experimental results on non-occluded Re-ID datasets. Finally, we conducted an ablation study to prove the effectiveness of each component.

Datasets

- **Occluded-Duke** (Miao et al. 2019a). It is a subset of DukeMTMC-reID (Ristani et al. 2016), which retains the occluded images in the source dataset. The Occluded-Duke contains 15618 training images, 2210 query images (all of them are occluded), and 17661 gallery images (some of them are occluded).
- **Partial-REID**. (Zheng et al. 2015b) It contains 600 images of 60 IDs for testing, 300 images for query, and 300 images for gallery. This dataset only provides the testing set, so we train our model on Market-1501 like other approaches.
- **Occluded-ReID** (Zhuo et al. 2018). This dataset contains 2000 images of 200 person captured by the mobile phone. The query set consists of 1000 occluded images (5 images for each person), and the gallery set contains 1000 non-occluded images of 200 person. This dataset only provides the testing set, so we train our model on Market-1501 like other approaches.
- **Market-1501** (Zheng et al. 2015a). The Market-1501 is a widely used non-occluded Re-ID dataset, which contains 1501 person captured by 6 cameras on campus. There are 12936 images (751 IDs) for training, and 21960 images (750 IDs, 19732 images in gallery, 2228 images in query) for testing.
- **DukeMTMC-reID** (Ristani et al. 2016). The Market-1501 is a well-known non-occluded Re-ID dataset, which contains 1404 person captured in 8 camera views. It contains 16522 training images and 19889 testing images.

Results on Occluded Re-ID

We compared our method with state-of-the-art occluded Re-ID methods on widely used occluded Re-ID datasets Occluded-Duke, Partial-REID and Occluded-ReID, including PCB (Sun et al. 2018), PGFA (Miao et al. 2019b), OAMN (Chen et al. 2021), MoS (Jia et al. 2021), ISP (Zhu et al. 2020), ViT Base (Dosovitskiy et al. 2020), PAT (Li et al. 2021), FED (Wang et al. 2022c), TransReID (He et al. 2021), and three methods using auxiliary clues HOREID (Wang et al. 2020), PVPM (Gao et al. 2020), PFD (Wang et al. 2022a).

As shown in Table 1, our method PADE achieves 63.0%/84.8% Rank-1 accuracy and 72.3%/89.3% mAP on Occluded-Duke and Partial-REID datasets, respectively, and the results outperforms both CNN-based and ViT-based methods. Moreover, the results of our PADE on Occluded-ReID are better than all the methods with no auxiliary clues. Because of the additional keypoint detection model, PFD (Wang et al. 2022a) performs slightly better than ours on mAP evaluation, but the Rank-1 accuracy of PFD is still 2.2% lower than ours.

The test set of these three datasets has a high proportion of occlusion data, which reaches 50% on Partial-REID

and Occluded-ReID. Therefore, it is difficult for both CNN-based and ViT-based methods to maintain the best accuracy on these datasets at the same time. Our PADE considers the data unbalanced problems in Re-ID and uses the parallel augmentation mechanism to improve the robustness of the network in the training phase. Therefore, the proposed method is able to maintain high accuracy on multiple datasets simultaneously and even outperforms the methods using auxiliary clues in most cases.

Results on non-occluded Re-ID

We choose two non-occluded Re-ID datasets, Market-1501 and DukeMTMC-reID, to evaluate our PADE and several state-of-the-art methods, including PGFA (Miao et al. 2019b), OAMN (Chen et al. 2021), MoS (Jia et al. 2021), ISP (Zhu et al. 2020), ViT Base (Dosovitskiy et al. 2020), PAT (Li et al. 2021), FED (Wang et al. 2022c), TransReID (He et al. 2021), HOREID (Wang et al. 2020) and PFD (Wang et al. 2022a).

From the Table 2, we can observe that the proposed PADE outperforms all the methods without using auxiliary clues and achieve higher results on Rank-1 accuracy compared with the state-of-the-art ViT-based PFD (Wang et al. 2022a) using extra pre-trained model. The person images in non-occluded Re-ID datasets have fewer occlusions, so the context in global features and details in local features can provide more useful information. The dual enhancement strategy helps our PADE to enhance and utilize both context and detailed information and achieve high accuracy.

Methods	Auxiliary Clues	Market-1501		DukeMTMC-reID	
		mAP	Rank-1	mAP	Rank-1
HOREID	✓	84.9	94.2	75.6	86.9
PFD [†]	✓	89.7	95.5	83.2	91.2
PGFA	×	76.8	91.2	65.5	82.6
OAMN	×	79.8	92.3	72.6	86.3
MoS	×	86.8	94.7	77.0	88.7
ISP	×	88.6	95.3	80.0	89.6
PAT [†]	×	88.0	95.4	78.2	88.8
FED [†]	×	86.3	95.0	78.0	89.4
TransReID [†]	×	88.9	95.2	82.0	90.7
Ours[†]	×	89.8	95.8	82.8	91.3

Table 2: Experimental results on Market-1501 and DukeMTMC-reID compared with state-of-the-art CNN-based and ViT-based methods (in %). [†] denotes the backbone of the method is ViT. The best results are shown in **blod**, the second results are shown in **blue**.

The majority of the data in the Market-1501 and DukeMTMC-reID test sets are non-occluded, with only a minor proportion of occlusion data. We manually implement erase and crop operations randomly on the test sets to simulate occluded data. The probability of a random crop operation is set to 1, and the probability of a random erase operation α is gradually increased from 0 to 1 (the interval is set to 0.2). The experimental results of ViT base, TransReID and our PADE under this setting are shown in Fig. 5.

We can observe that our PADE always achieves the best results and outperforms ViT base/TransReID on average by 15.3%/4.7% on mAP and outperforms ViT base/TransReID on average by 10.2%/4.1% on Rank-1 accuracy. It is worth noting that after α increases from 0 to 1, our method drops 12.3% and 8.4% in mAP and Rank-1, which is the least among the three methods, while transReID dropped by 13.1%/9%, ViT base dropped by 14%/12.8%. It means that our method suffers less when the occlusion data increases, and our model is more robust than the other two methods.

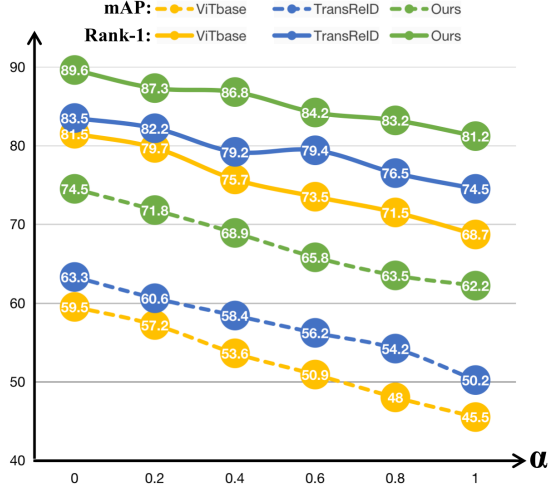


Figure 5: Experimental results of the proposed method, ViT base, and TransReID on different ratio of occluded data in DukeMTMC-reID. We manually implement occlusion and cropping on the test data, where α represents the probability of random erase operation.

Ablation Study

To prove the effectiveness of each component in the proposed method, we conduct the ablation study on Occluded-Duke by progressively introducing every component. The experimental results are shown in Table 3. The parallel augmentation mechanism changes the data preprocessing and generates two types of occlusion common in the test set. The model trained with the various occluded data achieves better results than the baseline, as shown in Table 3 (a) and (b). In addition, the dual enhancement strategy utilizes the context and details from the data itself, further improving the accuracy of the proposed method, as Table 3 (b) and (c) show.

Moreover, we replace the traditional augmentation in some methods with the proposed parallel augmentation mechanism. The experimental results are shown in Table 4. We choose the lightweight CNN-based baseline OSNet (Zhou et al. 2019), the vision transformer baseline ViT base (Dosovitskiy et al. 2020) and the latest ViT-based Re-ID baseline TransRe-ID (He et al. 2021) for experiment. We can observe that all methods gain improvement after using the parallel augmentation mechanism (PAM). By simply changing the form of data augmentation, PAM can improve TransReID by 2.3%/3.7% on mAP and Rank-1 accuracy.

Ablation Study	Modules		Occluded-Duke	
	PAM	DES	mAP	R-1
a)	-	-	57.3	67.8
b)	✓	-	62.7	71.8
c)	✓	✓	63.0	72.3

Table 3: Ablation study of the proposed method on Occluded-Duke (in %). **PAM**: Parallel Augmentation Mechanism. **DES**: Dual Enhancement Strategy.

Methods	Occluded-Duke	
	mAP	Rank-1
OSNet w/ NAM	29.5	38.1
OSNet w/ PAM	32.7 (+3.2)	42.5 (+4.4)
ViT base w/ NAM	52.3	59.9
ViT base w/ PAM	57.9 (+5.6)	66.2 (+6.3)
TransReID w/ NAM	60.4	68.1
TransReID w/ PAM	62.7 (+2.3)	71.8 (+3.7)

Table 4: Experimental results of our proposed Parallel Augmentation Mechanism (**PAM**) and Normal Augmentation Mechanism (**NAM**) on Occluded-Duke (in %).

To verify the effectiveness of *EraseAugmentation* and *CropAugmentation*, we conduct experiments while they work alone. According to Table 5 (b) and (c), implementing *EraseAugmentation* and *CropAugmentation* can improve mAP and Rank-1 accuracy by 3.9%/2.2% and 2.8%/1.7%, respectively.

	<i>EraseAugmentation</i>	<i>CroppingAugmentation</i>	Occluded-Duke	
			mAP	R-1
a)	-	-	57.3	67.8
b)	✓	-	61.2	70.0
c)	-	✓	60.1	69.5
d)	✓	✓	62.7	71.8

Table 5: Experimental results of different augmentations in the proposed Parallel Augmentation on Occluded-Duke (in %).

Conclusion

In this paper, we propose a simple but effective method with Parallel Augmentation and Dual Enhancement for robust performance on both occluded and non-occluded person Re-ID. The novel parallel augmentation mechanism (PAM) can generate the image triplet (including non-occluded, erased, and cropped images), and help the network gain better ability on occluded-agnostic test data. The context information and details in global and local features will promote each other according to dual enhancement strategy (DES). Both PAM and DES in our method can be flexibly embedded into other Re-ID methods, and they do not rely on any additional data annotations or models.

References

- Chen, P.; Liu, W.; Dai, P.; Liu, J.; Ye, Q.; Xu, M.; Chen, Q.; and Ji, R. 2021. Occlude them all: Occlusion-aware attention network for occluded person re-id. In *Proc. IEEE International Conference on Computer Vision*, 11833–11842.
- Ding, Y.; Sheng, L.; Liang, J.; Zheng, A.; and He, R. 2022. ProxyMix: Proxy-based Mixup Training with Label Refinery for Source-Free Domain Adaptation. *arXiv preprint arXiv:2205.14566*.
- Dosovitskiy, A.; Beyer, L.; Kolesnikov, A.; Weissenborn, D.; Zhai, X.; Unterthiner, T.; Dehghani, M.; Minderer, M.; Heigold, G.; Gelly, S.; et al. 2020. An image is worth 16x16 words: Transformers for image recognition at scale. *arXiv preprint arXiv:2010.11929*.
- Gao, S.; Wang, J.; Lu, H.; and Liu, Z. 2020. Pose-guided visible part matching for occluded person reid. In *Proc. IEEE Conference on Computer Vision and Pattern Recognition*, 11744–11752.
- He, S.; Luo, H.; Wang, P.; Wang, F.; Li, H.; and Jiang, W. 2021. Transreid: Transformer-based object re-identification. In *Proc. IEEE International Conference on Computer Vision*, 15013–15022.
- Huang, Z.; Liu, J.; Li, L.; Zheng, K.; and Zha, Z.-J. 2022. Modality-Adaptive Mixup and Invariant Decomposition for RGB-Infrared Person Re-Identification. In *Proc. AAAI Conference on Artificial Intelligence*.
- Jia, M.; Cheng, X.; Zhai, Y.; Lu, S.; Ma, S.; Tian, Y.; and Zhang, J. 2021. Matching on sets: Conquer occluded person re-identification without alignment. In *Proc. AAAI Conference on Artificial Intelligence*, volume 35, 1673–1681.
- Li, Y.; He, J.; Zhang, T.; Liu, X.; Zhang, Y.; and Wu, F. 2021. Diverse part discovery: Occluded person re-identification with part-aware transformer. In *Proc. IEEE Conference on Computer Vision and Pattern Recognition*, 2898–2907.
- Luo, C.; Song, C.; and Zhang, Z. 2020. Generalizing person re-identification by camera-aware invariance learning and cross-domain mixup. In *Proc. European Conference on Computer Vision*, 224–241. Springer.
- Miao, J.; Wu, Y.; Liu, P.; Ding, Y.; and Yang, Y. 2019a. Pose-guided feature alignment for occluded person re-identification. In *Proc. IEEE International Conference on Computer Vision*, 542–551.
- Miao, J.; Wu, Y.; Liu, P.; Ding, Y.; and Yang, Y. 2019b. Pose-guided feature alignment for occluded person re-identification. In *Proc. IEEE International Conference on Computer Vision*, 542–551.
- Ristani, E.; Solera, F.; Zou, R.; Cucchiara, R.; and Tomasi, C. 2016. Performance measures and a data set for multi-target, multi-camera tracking. In *Proc. European Conference on Computer Vision*, 17–35. Springer.
- Song, C.; Huang, Y.; Ouyang, W.; and Wang, L. 2018. Mask-guided contrastive attention model for person re-identification. In *Proc. IEEE Conference on Computer Vision and Pattern Recognition*, 1179–1188.
- Sun, Y.; Xu, Q.; Li, Y.; Zhang, C.; Li, Y.; Wang, S.; and Sun, J. 2019. Perceive where to focus: Learning visibility-aware part-level features for partial person re-identification. In *Proc. IEEE Conference on Computer Vision and Pattern Recognition*, 393–402.
- Sun, Y.; Zheng, L.; Yang, Y.; Tian, Q.; and Wang, S. 2018. Beyond part models: Person retrieval with refined part pooling (and a strong convolutional baseline). In *Proc. European Conference on Computer Vision*, 480–496.
- Wang, G.; Yang, S.; Liu, H.; Wang, Z.; Yang, Y.; Wang, S.; Yu, G.; Zhou, E.; and Sun, J. 2020. High-order information matters: Learning relation and topology for occluded person re-identification. In *Proc. IEEE Conference on Computer Vision and Pattern Recognition*, 6449–6458.
- Wang, G.; Yuan, Y.; Chen, X.; Li, J.; and Zhou, X. 2018. Learning discriminative features with multiple granularities for person re-identification. In *Proc. ACM International Conference on Multimedia*, 274–282.
- Wang, T.; Liu, H.; Song, P.; Guo, T.; and Shi, W. 2022a. Pose-guided Feature Disentangling for Occluded Person Re-identification Based on Transformer. In *Proc. AAAI Conference on Artificial Intelligence*, volume 36, 2540–2549.
- Wang, Z.; Li, C.; Zheng, A.; He, R.; and Tang, J. 2022b. Interact, Embed, and EnlargeE (IEEE): Boosting Modality-specific Representations for Multi-Modal Person Re-identification. In *Proc. AAAI Conference on Artificial Intelligence*.
- Wang, Z.; Zhu, F.; Tang, S.; Zhao, R.; He, L.; and Song, J. 2022c. Feature Erasing and Diffusion Network for Occluded Person Re-Identification. In *Proc. IEEE Conference on Computer Vision and Pattern Recognition*, 4754–4763.
- Xu, M.; Zhang, J.; Ni, B.; Li, T.; Wang, C.; Tian, Q.; and Zhang, W. 2020. Adversarial domain adaptation with domain mixup. In *Proc. AAAI Conference on Artificial Intelligence*, volume 34, 6502–6509.
- Ye, M.; Shen, J.; Lin, G.; Xiang, T.; Shao, L.; and Hoi, S. C. 2021. Deep learning for person re-identification: A survey and outlook. *IEEE Transactions on Pattern Analysis and Machine Intelligence*, 44: 2872–2893.
- Zhang, H.; Cisse, M.; Dauphin, Y. N.; and Lopez-Paz, D. 2017. mixup: Beyond empirical risk minimization. *arXiv preprint arXiv:1710.09412*.
- Zheng, L.; Shen, L.; Tian, L.; Wang, S.; Wang, J.; and Tian, Q. 2015a. Scalable person re-identification: A benchmark. In *Proc. IEEE International Conference on Computer Vision*, 1116–1124.
- Zheng, W.-S.; Li, X.; Xiang, T.; Liao, S.; Lai, J.; and Gong, S. 2015b. Partial person re-identification. In *Proc. IEEE International Conference on Computer Vision*, 4678–4686.
- Zhou, K.; Yang, Y.; Cavallaro, A.; and Xiang, T. 2019. Omni-scale feature learning for person re-identification. In *Proc. IEEE International Conference on Computer Vision*, 3702–3712.
- Zhu, K.; Guo, H.; Liu, Z.; Tang, M.; and Wang, J. 2020. Identity-guided human semantic parsing for person re-identification. In *Proc. European Conference on Computer Vision*, 346–363. Springer.

Zhuo, J.; Chen, Z.; Lai, J.; and Wang, G. 2018. Occluded person re-identification. In *Proc. IEEE International Conference on Multimedia and Expo*, 1–6.